NANO LETTERS
Letter
Cite This: Nano Lett. 2018, 18, 1535−1542
pubs.acs.org/NanoLett

# Phonon Driven Floquet Matter

Hannes Hübener,[†,‡,⊥] Umberto De Giovannini,[†,‡,⊥] and Angel Rubio[†,‡,§,*]

[†]Max Planck Institute for the Structure and Dynamics of Matter, Luruper Chaussee 149, 22761 Hamburg, Germany
[‡]Center for Free-Electron Laser Science and Department of Physics, University of Hamburg, Luruper Chaussee 149, 22761 Hamburg, Germany
[§]Center for Computational Quantum Physics (CCQ), The Flatiron Institute, 162 Fifth Avenue, New York, New York 22761, USA

Supporting Information

**ABSTRACT:** The effect of electron−phonon coupling in materials can be interpreted as a dressing of the electronic structure by the lattice vibration, leading to vibrational replicas and hybridization of electronic states. In solids, a resonantly excited coherent phonon leads to a periodic oscillation of the atomic lattice in a crystal structure bringing the material into a nonequilibrium electronic configuration. Periodically oscillating quantum systems can be understood in terms of Floquet theory, which has a long tradition in the study of semiclassical light-matter interaction. Here, we show that the concepts of Floquet analysis can be applied to coherent lattice vibrations. This coupling leads to phonon-dressed quasi-particles imprinting specific signatures in the spectrum of the electronic structure. Such dressed electronic states can be detected by time- and angular-resolved photoelectron spectroscopy (ARPES) manifesting as sidebands to the equilibrium band structure. Taking graphene as a paradigmatic material with strong electron−phonon interaction and nontrivial topology, we show how the phonon-dressed states display an intricate sideband structure revealing the electron−phonon coupling at the Brillouin zone center and topological ordering of the Dirac bands. We demonstrate that if time-reversal symmetry is broken by the coherent lattice perturbations a topological phase transition can be induced. This work establishes that the recently demonstrated concept of light-induced nonequilibrium Floquet phases can also be applied when using coherent phonon modes for the dynamical control of material properties.

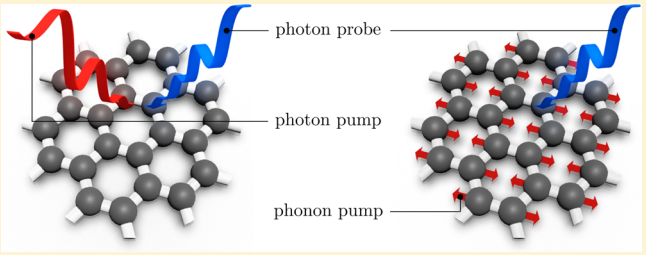


**KEYWORDS:** *First-principles calculations, photoelectron spectroscopy, nonequilibrium bandstructure, pumpprobe spectroscopy, Floquet theory, electron−phonon coupling*

Interaction of electrons and bosons in solids and molecules often leads to satellite features in the electronic structure resulting from harmonics of the boson mode. A well-known example are plasma oscillations in solids that are detectable as satellites in the photoelectron spectrum.[1,2] Another one is the effect of vibrational motion of ions that provides an intrinsic mode of the material that is detectable in the electronic structure, most prominently as vibrational sidebands in optical absorption spectroscopy of molecules.[3] In equilibrium, a strong electron−phonon coupling can result in a dressed electronic structure where the dressing creates observable replica bands[4−10] or kinks[11−13] in the electronic spectrum. In such a strongly coupled material, a few phonon quanta have a large effect on the electrons, whereas in a weaker coupled system one needs more quanta to achieve a similar effect. Creating more quanta of a boson mode means that one has to excite it coherently, thereby driving the system out of its equilibrium.

The controlled excitation of lattice vibrations as coherent phonon modes[14] has been shown to provide an avenue toward engineering long-lived, transient nonequilibrium states, such as light-enhanced[15] and light-induced superconductivity,[16] vibrationally controlled[17,18] and induced[19] magnetism, and phonon control of ferroelectricity[20] among others. This kind of nonequilibrium boson driven phases might also be used to affect exciton-[21] and polariton-condensates[22] and Higgs-modes superconductors.[23,24] In particular, the proposed ability to induce a superconducting phase in materials that are ordinary conductors in equilibrium by optically exciting coherent phonons[16,25−27] has spurred theoretical investigations into the electronic properties of materials under such nonequilibrium conditions.[28−30] Recently, the possibility to affect spin-polarization and magnetization through phonon-driving has been proposed for transition metal dichalcogenides.[31]

We show how the electronic structure together with the time-periodic ionic potential created by a coherent phonon mode can be interpreted as a steady state, quasi-static system when observed for times longer than the phonon time-scale. Such a Floquet state where the coherent phonon dresses the electronic states represents a distinct nonequilibrium phase with a fundamentally altered electronic structure. This kind of

Received: December 22, 2017
Revised: January 23, 2018
Published: January 23, 2018






DOI: 10.1021/acs.nanolett.7b05391
Nano Lett. 2018, 18, 1535−1542

nonequilibrium steady state picture of a dressed electronic structure has a long tradition when considering light-matter interaction, going back all the way to the idea of electrons being dressed by photons in the optical Stark effect.[32−37] However, recently there has been considerable activity in the theoretical framework of Floquet theory for light-driven matter following the proposal of the Floquet topological insulator.[38−43] The Floquet−phonon framework proposed here can be used as a paradigm to treat vibrationally excited systems and is thus, for example, also applicable for shaken optical lattices, where instead of a phonon mode a macroscopic vibration is applied.[44] It is equally applicable to the interpretation of vibrational spectroscopy in molecules, where the phonon-dressed sidebands occur as a series of vibrational peaks. Moreover, we posit that this framework is transferable to other coherent bosonic excitations that can be expressed as semiclassical fields such as plasmons or magnons.

In contrast to the interaction of optical light with electrons, where the massless photons dress the electrons with fast oscillating fields, the picture is reversed when considering the effect of a coherent phonon on the electronic structure. The relatively slow movement of the much heavier ions allows for the electrons to follow this movement almost instantaneously. Indeed, this picture gives rise to the frozen phonon approximation, where one assumes that the electrons experience any given ionic configuration of the lattice as if the lattice was fixed. While this approximation has been used successfully in a wide range of applications,[45−52] we show that it fails to accurately represent the electronic structure under the Floquet−phonon conditions. The frozen phonon approximation cannot account for the dynamical dressing effect that the coherently oscillating lattice supplies to the electronic structure. By using a first-principles Floquet description we show that one can define observable band structures of the dynamical system that are fundamentally different from the frozen phonon approach.

The failure of the frozen phonon approximation to correctly describe dynamical effects of the electron−phonon coupling in graphene has been pointed out before.[53] The lattice vibration dynamically changes the electronic structure, which in turn leads to a large renormalization of phonon modes. The Floquet−phonon approach presented here can serve as a starting point to compute such a dynamical renormalization of phonon energies, resulting in a nonequilibrium phonon bandstructure.

We present results obtained from two different complementary types of first-principles calculations, by first computing the real-time propagation of a quantum mechanical electronic system together with classical movement of the ions. In a second approach, we analyze the periodic oscillation induced by this motion with Floquet theory, thereby obtaining a quasi-static representation of the dynamics which allows us to explain in detail spectroscopic features of the time-evolution and analyze them in terms of the underlying multiphonon band structure. In this work, we are considering the in-plane double degenerate optical phonon of graphene as a paradigm for a coherently driven phonon system. While these modes are not infrared active in monolayer graphene, they can become active in bilayer graphene[54] and thus the features discussed here could be observed in this material. The features we discuss are generic for any semimetal and thus have readily transferable implications for driven charge-density wave and electron−phonon superconductors. The topology of the Dirac bands on the other hand is specific to topological systems and our results represent a general dynamically induced topological phase transition.

**Results.** To observe the effect of a coherent lattice motion on the electronic structure of graphene, we calculate the time- and angular-resolved photoelectron spectroscopy (ARPES) spectrum by using time-dependent density functional theory (TDDFT)[55,56] coupled to Ehrenfest molecular dynamics for the classical motion of the ions according to the optical $E_{2g}$ mode of graphene, c.f. Figure 1 and Materials and Methods for technical details. We assume that after an initial excitation of the coherent phonon the pump laser is switched off, but the phonon mode maintains its coherence for some time in which the system is probed. In our simulations, we use probe times of up to 160 fs which is well below reported coherence times for phonon modes of about 1 ps.[57] The resulting photoemission spectrum for a probe pulse longer than the $E_{2g}$ phonon period of 20.6 fs, corresponding to the frequency of this mode at the Γ-point of the phonon-Brillouin zone, is shown in Figure 1a.

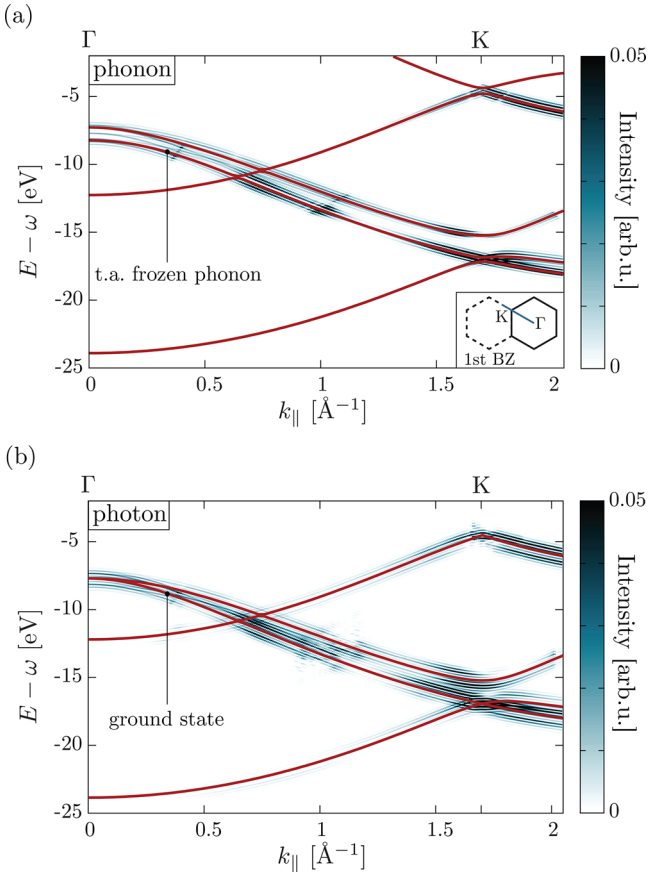


**Figure 1.** Time-resolved ARPES of graphene under different fundamental excitations: (a) The computed time-resolved ARPES spectrum of graphene under driving by a coherent the $E_{2g}$ optical phonon. In red is shown the frozen phonon band structure averaged over a phonon cycle (see text). (b) Under only optical excitations with fixed ions the time-resolved ARPES specturm displays a similar sideband splitting as the phonon-dressed system throughout the Brillouin zone but the strongly interacting pattern at the Γ-point is absent. In red is shown the ground-state bandstructure. The inset to (a) shows the path in momentum space that is chosen to cross the second Brillouin zone, because it provides a stronger photoelectron signal.



DOI: 10.1021/acs.nanolett.7b05391
Nano Lett. 2018, 18, 1535−1542

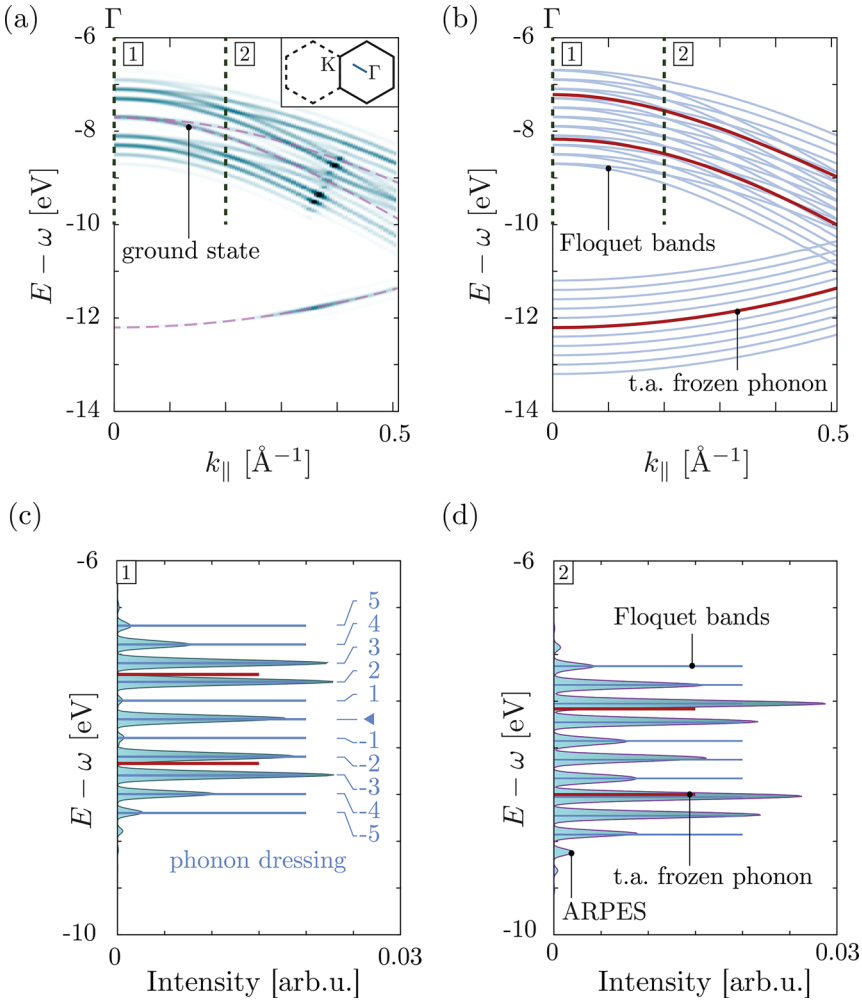


**Figure 2.** Time-resolved ARPES of graphene at the Γ-point with a coherent phonon: (a) Computed time-resolved ARPES spectrum of for a small path in the Γ-K direction of the Brillouin zone (see inset). An intricate sideband structure originating from the coherent phonon excitation is visible. (b) Band structure computed from Floquet analysis of the first-principles time-dependent Hamiltonian. In red is shown the time averaged frozen phonon band structure (see text) that can be seen failing to give the essential spectral features. (c,d) Vertical cuts through the time-resolved ARPES spectrum shown as dashed lines in (a) together with the Floquet energy levels taken at the same position, as indicated by the dashed lines in (b). In (c), the Floquet bands are indexed according to their phonon-multiplicity and the position of the original band is indicated by a triangle. Both cuts show the excellent agreement between the Floquet bands and the time-resolved ARPES spectrum. The low intensity of the first sidebands of the $\sigma$-bands at the Γ-point is due to weak photoelectron matrix elements. The cycle averaged frozen phonon bands (red) do not coincide either with Floquet levels nor with peaks in the calculated time-resolved ARPES spectrum.

We show photoelectron spectra for the second Brilluoin zone throughout this paper, because they display a stronger photoelectron signal. For comparison with the first Brillouion zone, see SI Figure S3. The frozen phonon picture assumes that at any given time the electrons are in the equilibrium corresponding to the lattice configuration at that time. This suggests, as an ad hoc approximation for the time-resolved ARPES spectrum, to take the average the different frozen-phonon band structures over the time of measurement. Such a time-averaged frozen-phonon band structure is shown for comparison with the time-resolved ARPES result in Figure 1a. By contrast, we show in Figure 1b the corresponding time-resolved ARPES spectrum where only an optical pump pulse is used and the ions are kept fixed in their equilibrium positions so that only the effect of photodressing is observed. The different behavior of the electronic structure is most striking at the Γ-point of the Brillouin zone. Overall the two different dressing mechanisms result in a similar structure that is characterized by an equally spaced stacking of sidebands around an equilibrium band. The degenerate top valence band at Γ, known as the $\sigma$-bands, however, display a qualitatively different behavior as becomes clear in Figure 2a. The photoelectron spectrum shows an apparent split electronic bands around the degenerate ground-state bands which seems to be in agreement with the cycle averaged frozen phonon band structure. This agreement, however, is deceptive and the underlying mechanism is more involved, as will become clear below, by considering the Floquet spectrum. Above all, we point out that a frozen phonon description lifts the degeneracy of the top valence band, which is clearly not observed in the photoelectron spectrum, where the position of the ground-state bands is preserved. Whereas in these calculations we consider only the specific lattice vibration associated with the coherent $E_{2g}$ phonon, we have also performed calculations with an additional random (thermal) distribution of ionic motion and find the same photoelectron spectrum (c.f SI Figure S1).

Although the cycle-averaged frozen-phonon bands seemingly capture the redistribution of the photoelectron spectral weights



DOI: 10.1021/acs.nanolett.7b05391
*Nano Lett.* 2018, 18, 1535−1542

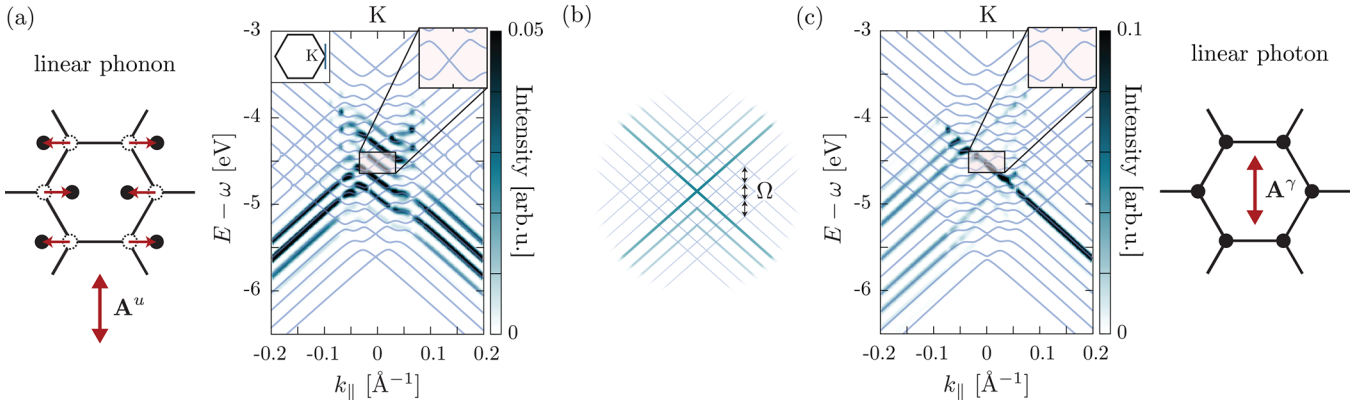


**Figure 3.** Time-resolved ARPES of graphene at the K-point with linearly polarized pumping. (a) The coherent phonon motion depicted in the sketch leads to a time-resolved ARPES spectrum that is very well described by the corresponding TDDFT−Floquet band structures. In particular, the degeneracy of the Dirac bands at the Dirac point can be seen to be preserved by Floquet theory (see inset). By contrast in (c) is shown the ARPES spectrum of a corresponding electronic structure where the ions are fixed and only the effect of a photon pump is included. Except for differences in the photoelectron intensities, the two dressing mechanism result in the same nonequilibrium electronic structure. The dynamical effect of the lattice perturbation on the electronic structure can be described by an effective gauge field, indicated by $A^u$, that plays the same role as the physical electromagnetic vector potential $A^\gamma$ of the photon field. Panel (b) indicates how to identify the sidebands in the band diagrams, as originating from a regular mesh of shited Dirac bands.

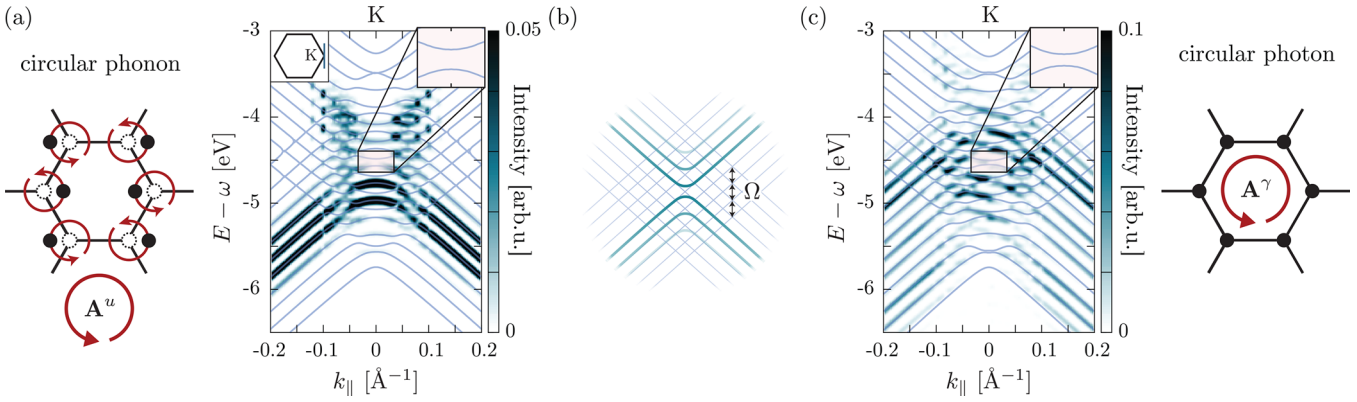


**Figure 4.** Time-resolved ARPES of graphene at the K-point with circularly polarized pumping. (a) The coherent phonon motion depicted in the sketch leads to a time-resolved ARPES spectrum that is very well described by the corresponding TDDFT−Floquet band structures. In particular the degeneracy of the Dirac points is lifted (see inset) and the system is in a nontrivial topological phase. (c) The corresponding time-resolved ARPES spectra where the ions are fixed and only the effect of photon-dressing is shown. While the time-resolved ARPES show different intensity patterns than for the corresponding phonon-dressed case, the Floquet band structures reveal that for the Dirac point the phonon- and the photon-dressing create the same kind of nonequilibrium phase. The dynamical effect of the lattice perturbation on the electronic structure can be described by an effective gauge field, indicated by $A^u$, that plays the same role as the physical electromagnetic vector potential $A^\gamma$ of the photon field. Panel (b) indicates how to identify the sidebands in the band diagrams, as originating from a regular mesh of shited Dirac bands and the induced opening of a gap at band crossing points.

qualitatively correctly, they do not contain any information about the sideband structure and fail to account for the central band in the photoelectron spectrum. To obtain the electronic structure underlying the bands observed in the photoemission spectrum we use Floquet analysis of the time-dependent Hamiltonian generated by the TDDFT calculation.[43] In this method, a stationary state is expanded into a basis of Fourier components of multiples of the mode frequency Ω: $|\Psi_\alpha(t)\rangle = \sum_m \exp(-i(\epsilon_\alpha + m\Omega)t)|u_m\rangle$, where $\epsilon_\alpha$ is the quasi-static Floquet band. With this ansatz, the time-dependent Schrödinger equation becomes an eigenvalue problem $\sum_n \mathcal{H}^{mn}|u_n\rangle = \epsilon_\alpha|u_m\rangle$ of the static Floquet Hamiltonian $\mathcal{H}^{mn} = \frac{\Omega}{2\pi}\int_{2\pi/\Omega} dt e^{i(m-n)\Omega t}H(t) + \delta_{mn}m\Omega$. The eigenstates of this Hamiltonian span a Hilbert space with the dimension of the original electronic Hilbert space times the multimode (photon or phonon) dimension. The contribution of the latter is in principle infinite but can be truncated to a number large enough to capture the interaction between sidebands (see, for instance, SI Figure S2). The spectrum of this Hamiltonian gives the band structure of the dressed quasiparticles.

Floquet theory provides the correct way of performing the quantum-mechanical time-average over a cycle period of a steady state oscillating system and thus represents the finite time duration of the ARPES probe.[39,58] We note that in order to include the time-dependent Hamiltonian of a system with moving ions into the Floquet integrals it is essential to use a generic representation, such as real-space grids or plane-waves. A local basis, like atomic-centered orbitals, or the Kohn−Sham eigenstate representation of the Hamiltonian cannot be used here, because it precludes the possibility to perform an integral over the Hamiltonian at different times. We also note that because of the low energy of the dressing field, we cannot use a high-frequency expansion that is otherwise convenient for



DOI: 10.1021/acs.nanolett.7b05391
Nano Lett. 2018, 18, 1535−1542

analytic treatments. The results of the Floquet−TDDFT calculation of the coherent-phonon excited electronic system is shown in Figure 2b and the excellent agreement between the Floquet bands and the time-resolved ARPES spectrum of Figure 2a is apparent.

The sidebands of the $\sigma$-bands does not follow an underlying splitting of the bands, contrary to what the ad hoc frozen phonon approximation suggests. Instead of a splitting of the bands, the degeneracy is preserved even for the sidebands and comparison with the Floquet spectrum reveals that the first two sidebands are surpressed by photoelectron matrix elements. In Figure 2c,d, the time-resolved ARPES intensity for these bands around Γ is given in more detail, showing the excellent quantitative agreement between Floquet theory and the time-resolved ARPES spectrum, as well the failure of the frozen-phonon approximation to quantitatively reproduce even the splitting of the spectral weight.

The necessity of Floquet theory to correctly describe the dynamical dressing becomes even clearer when looking at the K-point of the Brillouin zone. In graphene, the Dirac point at $K$ is of particular interest because here the electronic structure can be represented by the two-level Dirac Hamiltonian, reflecting the particular topological properties of the material. Figures 3 and 4 show an enlarged view of differently (phonon and photon) dressed electronic structures around $K$. By comparing the Floquet band structure of the $E_{2g}$ mode, Figure 3a with the one of a linearly polarized photon field, Figure 3c, we find that by choosing the appropriate amplitudes one can obtain identical band structures for both types of excitation. This remarkable agreement is a consequence of the same nature of the underlying electron-boson coupling. The insets in Figure 3a,c show that neither the photon nor the phonon perturbation leads to the creation of a bandgap at the Dirac point.

The analogy of photon and phonon dressing at the K-point can be further exploited by considering a coherent phonon excitation that is a linear combination of the two degenerate longitudinal (LO) and transverse (TO) modes of $E_{2g}$ to create a circular, time-reversal symmetry breaking motion in analogy to a circularly polarized electromagnetic (photon) field. Indeed, as shown in Figure 4a,c both circular excitations result again in identical band structures. In this case, as shown by the insets of Figure 4a,c, the perturbation leads to the creation of a dynamical gap. Such an excitation is described by the Haldane model[59] and can be associated with a topological phase transition. This dynamical opening of the gap is a general feature of a Floquet topological phase[39] in graphene which, as will become clear below, is also a property of the coherent lattice excited state. Here, we point out that the apparent similarity of the nonequilibrium electronic structure at the K-point of graphene for different bosonic excitations is a consequence the same underlying coupling mechanism of the Dirac bands.

**Discussion.** Using Floquet theory the similarities of the dressed electronic structure at the Dirac point can be traced back to the coupling between the electrons and the coherent boson fields. The coupling for the phonon case is described by electron−phonon matrix elements[60] of the $E_{2g}$ mode, while for the photon case is mediated by dipole matrix elements with polarization corresponding to the pump laser. To first order the coupling of electrons to a coherent boson field is given by the Hamiltonian $H(t) = \sum_i \epsilon_i c_i^\dagger c_i + \sum_i m_{i,j} c_i^\dagger c_j \hat{F}(t)$ where $c^\dagger$ and $c$ are the Fermionic creation and annihilation operators, $\epsilon$ are the energies of the uncoupled electrons, and $m$ are the electron-boson coupling matrix elements. $\hat{F} = a^\dagger + a$ is the coherent boson field, which corresponds to the classical limit of the quantized field, oscillating with the frequency Ω. In the case of phonons, this is the time-dependent lattice displacement, $\hat{F}(t) = \sin(\Omega t)$ along oscillation direction $\mathbf{u}$ of the phonon, whereas for photons it is the classical vector potential of the laser polarized in $\mathbf{A}^\gamma$ direction.

For the Dirac bands around K, the ground-state Hamiltonian can be written as a two level system $H_0^D = v_F(k_x\sigma_x + k_y\sigma_y)$, where $\sigma_i$ are Pauli matrices and $k_i$ are the in-plane components of the crystal momentum centered at the Dirac point.[59] Expanding the time-dependent (boson coupled) Hamiltonian in the eigenbasis of the ground-state Hamiltonian yields (c.f SI for details)

$$H_{\mathbf{k}}^D(t) = v_F|\mathbf{k}|\sigma_z + m[\cos(\theta_{\mathbf{k}})\sigma_z + \sin(\theta_{\mathbf{k}})\sigma_y]\sin(\Omega t) \quad (1)$$

The angle $\theta_{\mathbf{k}}$ is the angle between the polarization of the vector potential $\mathbf{A}^\gamma$ and the $\mathbf{k}$-vector for the electromagnetic (photon) excitation. For the phonon case instead, $\theta_{\mathbf{k}}$ is the angle between $\mathbf{k}$ and a vector $\mathbf{A}^u$ that is perpendicular to the phonon-polarization, that is, $\mathbf{A}^u \cdot \mathbf{u} = 0$. The Hamiltonian eq 1 is a particular representation of the Peierl's substitution describing weak coupling to a classical field, that is, where $\mathbf{k} \rightarrow \mathbf{k} - \mathbf{A}^i$. This becomes evident when considering the eigenvalues of this operator for fixed time: $E_{[t]}^{\pm} = \pm v_F|\mathbf{k} - \mathbf{A}_{[t]}^i|$. Here we have parametrized the time-dependence to emphasize that such instantaneous eigenvalues do not have any physical meaning for a vector potential. Nevertheless, it shows the effect of the dressing field, either photonic or phononic, on the electronic Hamiltonian as an effective gauge field in minimal coupling (Peierl's substitution) form. In particular, it shows that the lattice deformation induced by the phonon displacement $\mathbf{u}$ can be described by an effective gauge field $\mathbf{A}^u$ that plays precisely the same role in the time-dependent phonon-coupled Hamiltonian as the physical vector potential does for the photon coupling. Because the instantaneous eigenvalues of eq 1 do not have physical meaning, one has to turn to Floquet theory to relate these two different gauge fields to observable quantities. Indeed, performing Floquet analysis of the time-dependent Hamiltonian eq 1 gives a Floquet spectrum that is identical for the two bosonic excitations. They both only depend on $m$, the respective effective coupling strength.

It has been noted before that a lattice deformation of graphene can be described with an effective gauge field around the Dirac point[53,61,62] and the present work shows that this property also holds for dynamical phonons. By comparing the ARPES and Floquet spectra of the phonon-dressed electronic structure to the equivalent photon-dressed band structure in Figures 3 and 4 we find indeed that the different dressing mechanisms result in the same spectra. Most importantly, the results reported in Figure 4 show that such an effective gauge field creates the same nonequilibrium electronic structure as a physical vector potential. The coherent phonon modes we are considering here are Γ-phonons which implies that the gauge field that they induce is uniform across the crystal. This is in analogy to the dipole approximation used here to describe the photons via a uniform vector potential. However, the Floquet framework also holds for excitations with finite momentum transfers, that is, lattice vibrations that induce spatial variations larger than the unit cell.

The implications of the equivalent behavior are most striking when considering an excitation that breaks time-reversal symmetry. The Haldane model[59] predicts that the breaking



DOI: 10.1021/acs.nanolett.7b05391
Nano Lett. 2018, 18, 1535−1542

of time-reversal symmetry in graphene leads to the emergence of nontrivial topology, a Chern insulator. It has been shown that such a phase can indeed be created by circularly polarized lasers and the changes in the topological structure, Chern numbers, of the Dirac points have been identified with Floquet theory.[39] Figure 4a,c shows the time-resolved ARPES and Floquet band structure for circularly polarized phonons and photons. Agreement for the two different excitations is observed underlining the fact that both dressed electronic structures originate from the same kind of Dirac Hamiltonian and implying that circularly polarized coherent phonons can induce the same kind of change in the topological order as photon fields.

Having shown how Floquet analysis is required to understand the bosonic electron dressing at the Dirac point, we now consider what happens at the Γ-point, where the phonon-dressed electronic structure results in a strongly modified ARPES spectrum when compared to the equilibrium, c.f. Figure 2a. The apparent agreement of the cycle-averaged frozen phonon bands with the ARPES spectrum is misleading, because it wrongly displays a splitting of the degenerate $\sigma$-bands. In fact, as can be seen from the photoelectron spectrum and the underlying Floquet band structure, Figure 2a,b, there is no such splitting, but instead, the nonequilibrium bands are spread out in the usual sideband pattern, that is common for Floquet bands. Nevertheless, the phonon-quasiparticle dressing at this point is not a trivial process. The strong splitting of the cycle averaged frozen phonon bands at Γ originates from a strong electron−phonon coupling. In the Floquet−phonon average, however, this does not result in a splitting of bands but instead the bands appear around the equilibrium position. The fractional occupations of the Floquet sidebands, that is, the time-averaged projections of the Floquet-state on the ground-state,[63] for these bands is spread across a region of ∼10 sidebands (c.f. SI Figure S2a). That means that despite the appearance around the equilibrium position, there is a large interaction between the levels, corresponding to the large electron−phonon coupling. This results in the observed widespread of spectral weight, thus mimicking the frozen phonon positions. Indeed, the agreement of the frozen phonon bands with the time-resolved ARPES spectrum is purely coincidental and a result of photoelectron matrix elements. In an optical absorption experiment, the sidebands would appear as a series of satellite peaks, which the frozen phonon approximation would not be able to describe.

The classical trajectory approach we have chosen here to describe the phonon motion is appropriate for coherently excited phonons. When instead the electronic structure is dressed by quantized phonons, similar features could be observed, provided there is a strong electron−phonon coupling. The observations would be qualitatively similar, except that the quantum interaction does not result in uniformly distributed sidebands, similar to what is known for photon-dressed states in quantum optics.[64] The treatment of photons as classical lattice motion, also implies that in our calculation we are not completely accounting for electronic lifetime effects due to electron−phonon coupling. Similarly, our real-time propagation scheme also does not account for the long-range part of the electron−electron scattering. Thus, one can expect that in experimentally observed ARPES spectra the sidebands could display a larger broadening. Reported theoretical values for electron−electron and electron−phonon scattering mediated lifetime broadening are in the range of at most few tenths of millielectronvolts for graphene[65] and should therefore not impede observation of the sidebands. In general and for other materials, if lifetimes are short compared to the phonon energy the states would be difficult to observe.

**Conclusion.** We have demonstrated that the interacting electronic structure in the presence of a coherent phonon gives rise to complex photoelectron spectra that reflect a non-equilibrium state of the system that can be fundamentally different from the ground state. The underlying dynamical dressing process where the slow lattice motion creates additional energy levels for the electrons cannot be described by the frozen phonon approach despite the relatively large time-scale of the motion. Instead, the correct way to approach the electronic structure of such a system is Floquet theory, where the time-average of the measurement process is performed while accounting for the quantum-mechanical nature of the dynamical interactions. The Floquet−phonon approach shows that the dynamical effect of a coherent phonon can be the same as the perturbation with an photon field, showing the fundamental equivalence between the two bosonic excitations. From such a treatment of graphene emerges a rich sideband structure that reveals the strong electron−phonon coupling at the Brillouin zone center and nontrivial topology of the nonequilibrium phase. The access to the nonequilibrium electronic structure provided by this approach can serve as a starting point for further first-principles investigations of nonequilibrium effects of electron phonon coupling, for example, giving access to nonequilibrium phonon bandstructures.

Here, we have considered the example case of graphene to demonstrate the basic mechanism but the present approach is designed to investigate other semimetal systems, where the low energy splittings of phonon-dressing alters the Fermi-surface leading to complex changes in the material properties, for example by creating charge-density waves through finite momentum phonons or creating a nonequilibrium topological phase. Having shown the equivalence between photon and phonon excitations within this Floquet interpretation it can be expected that this general framework also applies to the coherent limit of other bosonic excitations such as magnons, plasmons, or excitons.

## ■ ASSOCIATED CONTENT

### Supporting Information

The Supporting Information is available free of charge on the ACS Publications website at DOI: 10.1021/acs.nanolett.7b05391.

Materials and methods and additional figures (PDF)

## ■ AUTHOR INFORMATION


### Corresponding Author

*E-mail: angel.rubio@mpsd.mpg.de.

### ORCID

Hannes Hübener: 0000-0003-0105-1427

Umberto De Giovannini: 0000-0002-4899-1304


### Author Contributions

⊥H.H. and U.D.G. contributed equally to this work.

### Notes

The authors declare no competing financial interest.



DOI: 10.1021/acs.nanolett.7b05391
Nano Lett. 2018, 18, 1535−1542

## ■ ACKNOWLEDGMENTS

We are grateful for illuminating discussions with I. Gierz, S. Aeschlimann, M. A. Sentef, and Th. Brumme. We acknowledge financial support from the European Research Council (ERC-2015-AdG-694097), Grupos Consolidados (IT578-13), and the European Unions Horizon 2020 Research and Innovation program under Grant Agreements 676580 (NOMAD) and 646259 (MOSTOPHOS).

## ■ REFERENCES

(1) Lischner, J.; Pálsson, G. K.; Vigil-Fowler, D.; Nemsak, S.; Avila, J.; Asensio, M. C.; Fadley, C. S.; Louie, S. G. *Phys. Rev. B: Condens. Matter Mater. Phys.* **2015**, *91*, 205113.
(2) Caruso, F.; Lambert, H.; Giustino, F. *Phys. Rev. Lett.* **2015**, *114*, 146404.
(3) Holland, D. M. P.; Shaw, D. A.; Hayes, M. A.; Shpinkova, L. G.; Rennie, E. E.; Karlsson, L.; Baltzer, P.; Wannberg, B. *Chem. Phys.* **1997**, *219*, 91−116.
(4) Lee, J. J.; Schmitt, F. T.; Moore, R. G.; Johnston, S.; Cui, Y. T.; Li, W.; Yi, M.; Liu, Z. K.; Hashimoto, M.; Zhang, Y.; Lu, D. H.; Devereaux, T. P.; Lee, D.-H.; Shen, Z.-X. *Nature* **2014**, *515*, 245−248.
(5) Moser, S.; Moreschini, L.; Jaćimović, J.; Barišić, O. S.; Berger, H.; Magrez, A.; Chang, Y. J.; Kim, K. S.; Bostwick, A.; Rotenberg, E.; Forró, L.; Grioni, M. *Phys. Rev. Lett.* **2013**, *110*, 196403.
(6) Chen, C.; Avila, J.; Frantzeskakis, E.; Levy, A.; Asensio, M. C. *Nat. Commun.* **2015**, *6*, 8585.
(7) Cancellieri, C.; Mishchenko, A. S.; Aschauer, U.; Filippetti, A.; Faber, C.; Barišić, O. S.; Rogalev, V. A.; Schmitt, T.; Nagaosa, N.; Strocov, V. N. *Nat. Commun.* **2016**, *7*, 10386.
(8) Wang, Z.; McKeown Walker, S.; Tamai, A.; Wang, Y.; Ristic, Z.; Bruno, F. Y.; de la Torre, A.; Riccò, S.; Plumb, N. C.; Shi, M.; et al. *Nat. Mater.* **2016**, *15*, 835−839.
(9) Nie, Y. F.; Di Sante, D.; Chatterjee, S.; King, P. D. C.; Uchida, M.; Ciuchi, S.; Schlom, D. G.; Shen, K. M. *Phys. Rev. Lett.* **2015**, *115*, 096405.
(10) Verdi, C.; Caruso, F.; Giustino, F. *Nat. Commun.* **2017**, *8*, 15769.
(11) Graf, J.; d'Astuto, M.; Jozwiak, C.; Garcia, D. R.; Saini, N. L.; Krisch, M.; Ikeuchi, K.; Baron, A. Q. R.; Eisaki, H.; Lanzara, A. *Phys. Rev. Lett.* **2008**, *100*, 227002.
(12) Siegel, D. A.; Hwang, C.; Fedorov, A. V.; Lanzara, A. *New J. Phys.* **2012**, *14*, 095006.
(13) Mazzola, F.; Wells, J. W.; Yakimova, R.; Ulstrup, S.; Miwa, J. A.; Balog, R.; Bianchi, M.; Leandersson, M.; Adell, J.; Hofmann, P.; Balasubramanian, T. *Phys. Rev. Lett.* **2013**, *111*, 216806.
(14) Först, M.; Manzoni, C.; Kaiser, S.; Tomioka, Y.; Tokura, Y.; Merlin, R.; Cavalleri, A. *Nat. Phys.* **2011**, *7*, 854−856.
(15) Hu, W.; Kaiser, S.; Nicoletti, D.; Hunt, C. R.; Gierz, I.; Hoffmann, M. C.; Le Tacon, M.; Loew, T.; Keimer, B.; Cavalleri, A. *Nat. Mater.* **2014**, *13*, 705−711.
(16) Mitrano, M.; Cantaluppi, A.; Nicoletti, D.; Kaiser, S.; Perucchi, A.; Lupi, S.; Di Pietro, P.; Pontiroli, D.; Riccò, M.; Clark, S. R.; Jaksch, D.; Cavalleri, A. *Nature* **2016**, *530*, 461−464.
(17) Rini, M.; Tobey, R.; Dean, N.; Itatani, J.; Tomioka, Y.; Tokura, Y.; Schoenlein, R. W.; Cavalleri, A. *Nature* **2007**, *449*, 72−74.
(18) Först, M.; Caviglia, A. D.; Scherwitzl, R.; Mankowsky, R.; Zubko, P.; Khanna, V.; Bromberger, H.; Wilkins, S. B.; Chuang, Y. D.; Lee, W. S.; et al. *Nat. Mater.* **2015**, *14*, 883−888.
(19) Nova, T. F.; Cartella, A.; Cantaluppi, A.; Först, M.; Bossini, D.; Mikhaylovskiy, R. V.; Kimel, A. V.; Merlin, R.; Cavalleri, A. *Nat. Phys.* **2017**, *13*, 132−136.
(20) Mankowsky, R.; von Hoegen, A.; Först, M.; Cavalleri, A. *Phys. Rev. Lett.* **2017**, *118*, 197601.
(21) Kasprzak, J.; Richard, M.; Kundermann, S.; Baas, A.; Jeambrun, P.; Keeling, J. M. J.; Marchetti, F. M.; nacute, M. H. S.; ska; André, R.; Staehli, J. L.; Savona, V.; Littlewood, P. B.; Deveaud, B.; Dang, L. S. *Nature* **2006**, *443*, 409−414.
(22) Cerda-Méndez, E. A.; Krizhanovskii, D. N.; Wouters, M.; Bradley, R.; Biermann, K.; Guda, K.; Hey, R.; Santos, P. V.; Sarkar, D.; Skolnick, M. S. *Phys. Rev. Lett.* **2010**, *105*, 116402.
(23) Matsunaga, R.; Tsuji, N.; Fujita, H.; Sugioka, A.; Makise, K.; Uzawa, Y.; Terai, H.; Wang, Z.; Aoki, H.; Shimano, R. *Science* **2014**, *345*, 1145−1149.
(24) Sherman, D.; Pracht, U. S.; Gorshunov, B.; Poran, S.; Jesudasan, J.; Chand, M.; Raychaudhuri, P.; Swanson, M.; Trivedi, N.; Auerbach, A.; Scheffler, M.; Frydman, A.; Dressel, M. *Nat. Phys.* **2015**, *11*, 188−192.
(25) Först, M.; Tobey, R. I.; Bromberger, H.; Wilkins, S. B.; Khanna, V.; Caviglia, A. D.; Chuang, Y. D.; Lee, W. S.; Schlotter, W. F.; Turner, J. J.; et al. *Phys. Rev. Lett.* **2014**, *112*, 157002.
(26) Kaiser, S.; Clark, S. R.; Nicoletti, D.; Cotugno, G.; Tobey, R. I.; Dean, N.; Lupi, S.; Okamoto, H.; Hasegawa, T.; Jaksch, D.; Cavalleri, A. *Sci. Rep.* **2015**, *4*, 17.
(27) Mankowsky, R.; Subedi, A.; Först, M.; Mariager, S. O.; Chollet, M.; Lemke, H. T.; Robinson, J. S.; Glownia, J. M.; Minitti, M. P.; Frano, A.; et al. *Nature* **2014**, *516*, 71−73.
(28) Kennes, D. M.; Wilner, E. Y.; Reichman, D. R.; Millis, A. J. *Nat. Phys.* **2017**, *13*, 479.
(29) Sentef, M. A. *Phys. Rev. B: Condens. Matter Mater. Phys.* **2017**, *95*, 205111.
(30) Babadi, M.; Knap, M.; Martin, I.; Refael, G.; Demler, E. *Phys. Rev. B* **2017**, *96*, 014512.
(31) Shin, D.; Hübener, H.; De Giovannini, U.; Jin, H.; Rubio, A.; Park, N. *Nat. Commun.* **2018**, 10.1038/s41467-018-02918-5 (in press).
(32) Autler, S. H.; Townes, C. H. *Phys. Rev.* **1955**, *100*, 703−722.
(33) Shirley, J. H. *Phys. Rev.* **1965**, *138*, B979−B987.
(34) Fainshtein, A. G.; Manakov, N. L.; Rapoport, L. P. *J. Phys. B: At. Mol. Phys.* **1978**, *11*, 2561−2577.
(35) Grifoni, M.; Hänggi, P. *Phys. Rep.* **1998**, *304*, 229−354.
(36) Sie, E. J.; McIver, J. W.; Lee, Y.-H.; Fu, L.; Kong, J.; Gedik, N. *Nat. Mater.* **2015**, *14*, 290−294.
(37) De Giovannini, U.; Hübener, H.; Rubio, A. *Nano Lett.* **2016**, *16*, 7993−7998.
(38) Lindner, N. H.; Refael, G.; Galitski, V. *Nat. Phys.* **2011**, *7*, 490−495.
(39) Sentef, M. A.; Claassen, M.; Kemper, A. F.; Moritz, B.; Oka, T.; Freericks, J. K.; Devereaux, T. P. *Nat. Commun.* **2015**, *6*, 7047.
(40) Claassen, M.; Jia, C.; Moritz, B.; Devereaux, T. P. *Nat. Commun.* **2016**, *7*, 13074.
(41) Fleury, R.; Khanikaev, A. B.; Alù, A. *Nat. Commun.* **2016**, *7*, 11744.
(42) Zou, J.-Y.; Liu, B.-G. *Phys. Rev. B: Condens. Matter Mater. Phys.* **2016**, *93*, 205435.
(43) Hübener, H.; Sentef, M. A.; De Giovannini, U.; Kemper, A. F.; Rubio, A. *Nat. Commun.* **2017**, *8*, 13940.
(44) Choi, S.; Choi, J.; Landig, R.; Kucsko, G.; Zhou, H.; Isoya, J.; Jelezko, F.; Onoda, S.; Sumiya, H.; Khemani, V.; von Keyserlingk, C.; Yao, N. Y.; Demler, E.; Lukin, M. D. *Nature* **2017**, *543*, 221−225.
(45) Harmon, B. N.; Weber, W.; Hamann, D. R. *Le Journal de Physique Colloques* **1981**, *42*, C6-628−C6-630.
(46) Kunc, K.; Martin, R. M. *Phys. Rev. B: Condens. Matter Mater. Phys.* **1981**, *24*, 2311−2314.
(47) Weyrich, K. H. *Ferroelectrics* **1990**, *104*, 183−194.
(48) Van Dyck, D. *Ultramicroscopy* **2009**, *109*, 677−682.
(49) Budai, J. D.; Hong, J.; Manley, M. E.; Specht, E. D.; Li, C. W.; Tischler, J. Z.; Abernathy, D. L.; Said, A. H.; Leu, B. M.; Boatner, L. A.; McQueeney, R. J.; Delaire, O. *Nature* **2014**, *515*, 535−539.
(50) Novelli, F.; Giovannetti, G.; Avella, A.; Cilento, F.; Patthey, L.; Radovic, M.; Capone, M.; Parmigiani, F.; Fausti, D. *Phys. Rev. B: Condens. Matter Mater. Phys.* **2017**, *95*, 174524.
(51) Mann, A.; Baldini, E.; Tramontana, A.; Pomjakushina, E.; Conder, K.; Arrell, C.; van Mourik, F.; Lorenzana, J.; Carbone, F. *Phys. Rev. B: Condens. Matter Mater. Phys.* **2015**, *92*, 035147.
(52) Rossi, D.; Camacho-Forero, L. E.; Ramos-Sánchez, G.; Han, J. H.; Cheon, J.; Balbuena, P.; Son, D. H. *J. Phys. Chem. C* **2015**, *119*, 7436−7442.



DOI: 10.1021/acs.nanolett.7b05391
*Nano Lett.* 2018, 18, 1535−1542

(53) Pisana, S.; Lazzeri, M.; Casiraghi, C.; Novoselov, K. S.; Geim, A. K.; Ferrari, A. C.; Mauri, F. *Nat. Mater.* **2007**, *6*, 198−201.
(54) Gierz, I.; Mitrano, M.; Bromberger, H.; Cacho, C.; Chapman, R.; Springate, E.; Link, S.; Starke, U.; Sachs, B.; Eckstein, M.; Wehling, T. O.; Katsnelson, M. I.; Lichtenstein, A.; Cavalleri, A. *Phys. Rev. Lett.* **2015**, *114*, 125503.
(55) Runge, E.; Gross, E. K. U. *Phys. Rev. Lett.* **1984**, *52*, 997−1000.
(56) Bertsch, G. F.; Iwata, J. I.; Rubio, A.; Yabana, K. *Phys. Rev. B: Condens. Matter Mater. Phys.* **2000**, *62*, 7998−8002.
(57) Jeong, T.; Jung, S.; Yee, K. Coherent phonon dynamics in single-layer and multilayer graphene. *2015 11th Conference on Lasers and Electro-Optics Pacific Rim, CLEO-PR 2015*. 2016; pp 1−2 doi.org/10.1109/CLEOPR.2015.7375970
(58) De Giovannini, U.; Hübener, H.; Rubio, A. *J. Chem. Theory Comput.* **2017**, *13*, 265−273.
(59) Haldane, F. D. M. *Phys. Rev. Lett.* **1988**, *61*, 2015−2018.
(60) Giustino, F. *Rev. Mod. Phys.* **2017**, *89*, 015003.
(61) Sasaki, K.-i.; Saito, R. *Prog. of Theor. Phys. Supp.* **2008**, *176*, 253−278.
(62) Pereira, V. M.; Neto, A. H. C.; Peres, N. M. R. *Phys. Rev. B: Condens. Matter Mater. Phys.* **2009**, *80*, 045401.
(63) Oka, T.; Aoki, H. *J. Phys. Conf. Ser.* **2011**, *334*, 012060.
(64) Cohen-Tannoudji, C.; Haroche, S. *J. Phys. (Paris)* **1969**, *30*, 153−168.
(65) Park, C.-H.; Giustino, F.; Cohen, M. L.; Louie, S. G. *Phys. Rev. Lett.* **2007**, *99*, 086804.



DOI: 10.1021/acs.nanolett.7b05391
*Nano Lett.* 2018, 18, 1535−1542